This is the accepted manuscript version of the contribution published as:

Boumaiza, L., Walter, J., Chesnaux, R., Zahi, F., Huneau, F., Garel, E., Stotler, R.L., Bordeleau, G., Bordeleau, K.H., Vystavna, Y., Drias, T., Re, V., **Knöller, K.**, Stumpp, C. (2022):
Combined effects of seawater intrusion and nitrate contamination on groundwater in coastal agricultural areas: A case from the Plain of the El-Nil River (North-Eastern Algeria)
Sci. Total Environ. **851, Part 1** , art. 158153

The publisher's version is available at:

http://dx.doi.org/10.1016/j.scitotenv.2022.158153

Lamine Boumaiza[1,2], Julien Walter[1,2], Romain Chesnaux[1,2], Faouzi Zahi[3], Frédéric Huneau[4,5], Émilie Garel[4,5], Randy L. Stotler[6], Geneviève Bordeleau[7], Karen H. Johannesson[8], Yuliya Vystavna[9], Tarek Drias[10], Viviana Re[11], Kay Knöller[12], Christine Stumpp[13]

[1] Université du Québec à Chicoutimi, Département des Sciences Appliquées, Saguenay (Québec), G7H 2B1, Canada

[2] Centre d'études sur les ressources minérales, Groupe de recherche Risque Ressource Eau, Saguenay (Québec), G7H 2B1, Canada

[3] Université Mohammed Seddik Ben Yahia, Département des Sciences de la Terre et de l'Univers, Jijel, 18000, Algeria

[4] Université de Corse Pascal Paoli, Département d'Hydrogéologie, Campus Grimaldi, Corte, 20250, France

[5] CNRS, UMR 6134 SPE, Corte, 20250, France

[6] University of Waterloo, Department of Earth and Environmental Sciences, Waterloo (Ontario), N2T 0A4, Canada

[7] Institut national de la recherche scientifique, Centre Eau Terre Environnement, Québec (Québec) G1K 9A9, Canada

[8] University of Massachusetts Boston, School for the Environment, Boston, MA, 02125, USA

[9] International Atomic Energy Agency, Isotope Hydrology Section, Vienna, 1400, Austria

[10] Université Mustapha Benboulaïd, Département de Géologie, Campus de Fesdiss, 05030 Batna, Algeria

[11] University of Pisa, Department of Earth Sciences, Pisa, 56126, Italy

[12] Helmholtz Centre for Environmental Research, Department of Catchment Hydrology, Halle (Saale), 06120, Germany

[13] University of Natural Resources and Life Sciences, Institute of Soil Physics and Rural Water Management, Vienna, 1190, Austria

Combined effects of seawater intrusion and nitrate contamination on groundwater in coastal agricultural areas: A case from the Plain of the El-Nil River (North-Eastern Algeria)

Abstract (300 words max.)

This study focuses on coastal aquifers subject to uncontrolled land use development by investigating the combined effects of seawater intrusion and nitrate contamination. The research is undertaken in a Mediterranean coastal agricultural area (Plain of the El-Nil River, Algeria), where water resources are heavily impacted by anthropogenic activities. A multi-tracer approach, integrating hydrogeochemical and isotopic tracers (δ^2H_{H2O}, $\delta^{18}O_{H2O}$, $\delta^{15}N_{NO3}$ and $\delta^{18}O_{NO3}$), is combined with a hydrochemical facies evolution diagram, and a Bayesian isotope mixing model (MixSIAR) to assess seawater contamination with its inland intrusion, and distinguish the nitrate sources and their apportionment. Results show that seawater intrusion is circumscribed to the sector neighbouring the Mediterranean Sea, with two influencing functions including classic inland intrusion through the aquifer, and upstream seawater impact through the river mouth connected to the Mediterranean Sea. Groundwater and surface water samples reveal nitrate concentrations above the natural baseline threshold, suggesting anthropogenic influence. Results from nitrate isotopic composition, NO_3 and Cl concentrations, and the MixSIAR model show that nitrate concentrations chiefly originate from sewage and manure sources. Nitrate derived from the sewage is related to wastewater discharge, whereas nitrate derived from the manure is attributed to an excessive use of animal manure to fertilise agricultural areas. The dual negative impact of seawater intrusion and nitrate contamination degrades water quality over a large proportion of the study area. The outcomes of this study are expected to contribute to effective and sustainable water resources management in the Mediterranean coastal area. Furthermore, this study may improve scientists' ability to predict the combined effect of various anthropogenic stressors on coastal environments and help decision-makers elsewhere to prepare suitable environmental strategies for other regions currently undergoing an early stage of water resources deterioration.

Keywords

Seawater intrusion, Nitrate contamination, Stable isotopes, Aquifer, HFE-D, MixSIAR

1 Introduction

In many coastal areas, groundwater anthropogenic stressors are mainly related unsafe industrial/agricultural practices and uncontrolled urbanization, which commonly leads to seawater intrusion due to intensive groundwater pumping (Boumaiza et al., 2020; Gilabert-Alarcón et al., 2018; Madioune et al., 2014). Unsafe agricultural practices can negatively affect groundwater quality due to excessive use of fertilizers that are added to promote crops growth, combined with return flow of irrigation water (Lasagna and De Luca, 2017; Merchan et al., 2020; Pulido-Bosch et al., 2018). The effect of unsafe agricultural practices on groundwater has motivated several studies to investigate the sources, distribution, and impacts of contamination over various physiographical areas (Blarasin et al., 2020; Boumaiza et al., 2020; Stoewer et al., 2015). In particular, nitrate (NO_3) has received significant attention due to the negative adverse effects on human health and the environment (Anornu et al., 2017; Blaisdell et al., 2019). For example, excessive consumption of NO_3 in drinking water may lead to health problems, including methemoglobinemia "blue baby syndrome" in infants, colorectal and stomach cancer, spontaneous abortion, thyroid disorder, and neural tube defects in adults (Schroeder et al., 2020; Ward et al., 2018). From an environmental perspective, the discharge of NO_3 into surface water bodies can lead to eutrophication in coastal and marine environments, leading to considerable reduction of aquatic life (Gomez Isaza et al., 2020; Yeshno et al., 2019). Furthermore, partial denitrification of NO_3 releases nitrous oxide gas, which is a powerful greenhouse gas contributing to climate change (Sutton et al., 2011). It is generally recognized that agricultural practices are a primary source of NO_3 in groundwater, as the excessive use of synthetic/organic fertilizers in agricultural lands has been found to contribute up to 80% of the worldwide reactive produced nitrogen (Erisman et al., 2008). However, NO_3 can be provided by other anthropogenic sources, including wastewater discharges from septic tanks, leaking sewers, and landfill seepage (Boumaiza et al., 2020; Matiatos, 2016; Puig et al., 2017; Vystavna et al., 2017).

Uncontrolled urbanization in coastal environments can negatively affect groundwater quality in a variety of ways. For example, groundwater quality degradation can be caused by the discharge of untreated urban wastewater and improper waste disposal practices, which are common in rapidly growing urban areas in developing regions (Boumaiza et al., 2020; Elmeknassi et al., 2022; Re et al., 2014). Urbanization leads to increasingly intensive extraction of groundwater from local coastal aquifers, disturbing the "equilibrium" between fresh and saltwater, causing seawater intrusion and thus degrading groundwater quality (Bear et al., 1999). The seawater intrusion phenomenon is recognised as a major environmental problem in many coastal areas worldwide (Barry, 2016; Boumaiza et al., 2020; Shi and Jiao, 2014), and is particularly accentuated in areas where climate change causes other synergetic effects such as sea level rise and coastal erosion (Chesnaux et al., 2021). With 1% mixing of seawater into fresh groundwater (resulting in ≈ 250 mg/L chloride), the taste of groundwater becomes significantly affected, and it may be perceived as unsuitable for drinking (WHO, 2017). This negative effect is long-lasting, as the intruded saltwater within the inland aquifer requires decades to centuries to be flushed with freshwater (Bear et al., 1999; Foster and Chilton, 2003). Seawater intrusion, potentially combined with soil salinization, not only degrades groundwater quality, but also contributes to transformation of traditionally agricultural arable lands to useless saline areas with vegetation degradation and reduced crop yields (Arslan and Demir, 2013; Shi and Jiao, 2014).

Many studies in coastal areas have focused on seawater intrusion or nitrate contamination issues (Dhakate et al., 2020; Kaown et al., 2021; Kwon et al., 2021; Najib et al., 201; Obeidat et al., 2021; Re and Sacchi, 2017), whereas only limited number of investigations have tried to understand the combined effects of seawater intrusion and nitrate contamination in coastal agricultural areas. Although necessary for efficient and sustainable water resources management, studies considering both issues are challenging due to the multiple anthropogenic stressors impacting coastal agricultural areas. To fill in some of the remaining knowledge gaps —helping to establish efficient and sustainable water resources management of coastal agricultural areas— experimental studies are still needed. The present study provides a field-experimental research program guided along Mediterranean coastal agricultural area (i.e., the Plain of the El-Nil River, Algeria), where the water resources are heavily impacted by multiple anthropogenic stressors (Boufekane, 2017). This study provides an opportunity to quantify the challenges faced by many coastal areas around the world, especially in regions with uncontrolled development strategies.

The growth of agricultural activities over the Plain of the El-Nil River has generated uncontrolled drilling of an excessive number of private wells by local farmers. In addition, over-pumping of groundwater from the aquifer is related to high freshwater demand by an increasing population (Amiour, 2015; Bechkit, 2005; Berkane, 2011). As a consequence of excessive groundwater exploitation, an advancing seawater wedge towards the inland aquifer of the Plain of the El-Nil-River is expected. Locally elevated groundwater electrical conductivity (EC) values, ranging from 800 to 2,400 µS/cm, have been assumed as result of seawater intrusion (Amiour 2015, Boufekane 2017). However, the spatial extent of the seawater intrusion remains unknown. Therefore, the first objective of the present study consists to assess the seawater contamination and extent of intrusion owing to over-pumping of the aquifer. Major chemical ions and stable isotopes of the water (δ^2H_{H2O} and $\delta^{18}O_{H2O}$) were shown to be suitable to study the seawater intrusion issue, because they are able to give insights into the source of water and the main processes governing groundwater quality such as mixing and evaporation processes (Boumaiza et al., 2020; Santoni et al., 2018). Furthermore, the link between major ions and stable isotopes of water is highly reliable and a commonly used tool to investigate the origin of salinity (Dhakate et al., 2020; Elmeknassi et al., 2022; Mahlknecht et al., 2017).

Chemical analyses of groundwater samples collected in 2012 and 2014 revealed NO_3 concentrations above the natural baseline threshold of 5 mg/L (Appelo and Postma, 2005; Panno et al., 2006), suggesting an anthropogenic influence (Amiour, 2015; Boufekane, 2017). Both Amiour (2015) and Boufekane (2017) hypothesized the extensive use of fertilizers in the region was the source of the elevated groundwater NO_3 concentrations. However, this has not been verified using more conclusive tools, such as stable isotope-based methods or statistical-based approaches. The perennial rivers crossing the Plain of the El-Nil River receive wastewaters from sanitation networks of the neighboring urban communities (Boumaiza et al., 2021; Drouiche et al., 2022), and inadequate private sanitation systems are still operated by some residences who are unable to connect to the existing sanitation networks. These features suggest that high NO_3 concentrations in local groundwater could also be attributed to wastewater/sewage influx. Therefore, the second objective of the present study consists to distinguish the anthropogenic sources of nitrate and to estimate their apportionments in water system. Identifying nitrate sources is challenging due to a broad variety of potential anthropogenic sources. Nonetheless, stable isotopes of nitrate ($\delta^{15}N_{NO3}$ and $\delta^{18}O_{NO3}$) can be used to investigate nitrate sources (Pastén-Zapata et al., 2014; Stoewer et al., 2015). The benefit from using these stable isotopes resides in the expectation that some of the major nitrogen sources, involved in the terrestrial nitrogen cycle, have distinct isotope signatures in groundwater (Kendall et al., 2007).

Ultimately, the outcomes of the present study are expected to contribute to effective and sustainable natural resource management for the Plain of the El-Nil River. Furthermore, this study may improve scientists' ability to predict the combined effect of various anthropogenic stressors on coastal environments and help groundwater managers elsewhere to prepare suitable environmental plans for coastal regions undergoing an early stage of groundwater quality degradation.

2 Description of the study area

2.1 *Geographic location and climate*

The study area is a coastal agricultural plain located in the El-Tahir region of the Province of Jijel in northeastern Algeria (Fig. 1). It is crossed by the El-Nil River, flowing south to north, from which the plain was named the "Plain of the El-Nil River". Two other tributary rivers bordering the study area, the Boukaraa River and the Sayoud River, are connected to the El-Nil River. Also, there is a small surface water body (0.3 km^2), feeding from the Tassift River, which also feeds into the El-Nil River before the El-Nir River finally debouches into the Mediterranean Sea to the north (Fig. 1). The Plain of the El-Nil River, which covers a surface area of around 60 km^2, consists of an alluvial valley bottom surrounded by metamorphic mountains with elevations of between 100−400 m above sea level (a.s.l) (Fig. 1). The study area has a sub-humid Mediterranean climate featuring a mild winter with monthly average temperatures of 10.8 °C and hot summer with monthly average temperature of 27.5 °C. The study area is mainly fed by direct rainfall, which is estimated at an annual average of 1,000 mm, runoff from surrounding mountains, and potential water influx from the rivers crossing the study area (Boufekane, 2017; Mahdid et al., 2022).

Groundwater sample   Surface water sample

Fig. 1. Perspective overview of study area with and location of groundwater samples and surface water samples collected over the study area. Surface water samples were collected from the Tassift River (#2), the Boukaraa River (#5 and #6), the El-Nil River (#1, #3 and #4), the Sayoud River (#7), and the Mediterranean Sea (#35). In dashed red is the approximate limit of the study area.

2.2 *Geology and hydrogeological background*

The study area is an alluvial valley belonging to the Little Kabylia "*Petite Kabylie*" region, which comprises the northeastern Algerian coastal magmatic chain. The coastal magmatic chain outcrops from the Province of Jijel in the west to the Province of Annaba in the east, and extends south to the magmatic range of the El-Babor Mountains (Bouillin and Kornprobst, 1974; Durand, 1969). The Algerian coastal magmatic chain formed during the main paroxysmal compressional phases of the Eocene, Miocene, and Quaternary periods (Letouzey and Trémolières, 1980; Vila, 1980). Diverse Miocene and Quaternary deposits are exposed in the study area including sand, gravel, pebble, clay, silt, conglomerate, and marl surface deposits (Fig. 2). The corresponding plain and associated terraces consist of Quaternary alluvial deposits that are chiefly composed of sandy clay with a sandy shoreline band (Durozoy, 1954). Underlying the surficial sandy alluvial deposits are Quaternary granular alluvium deposits, varying in thickness between 20 and 80 m, overlying a Miocene marl substratum (CGG, 1971) (Fig. 2). The latter is about 50 m in thick under the Plain of the El-Nil River, and outcrops at the west of the study area where El-Tahir City is located (Fig. 2). The marl substratum overlies Paleozoic metamorphic bedrock basement (Permian–Triassic extinction) consisting of gneiss and schist (Messadi, 1992). The Plain of El-Nil River overlies a permeable unconsolidated aquifer featuring hydraulic conductivity varying between 2.32×10^{-3} and 3.58×10^{-3} m/s (Boufekane et al., 2019). The study area has been assigned with four vulnerability levels to contamination based on a DRASTIC index (Aller et al., 1987). A zone with low vulnerability to contamination, representing 10% of the study area, was identified at the edges of the Plain of the El-Nil River, whereas a second zone, occupying the upstream sectors of the study area (61%), was assigned with average vulnerability level. A third zone with high vulnerability level (26%) was identified along the El-Nil River and its tributaries, where the alluvial terraces are dominant. A fourth zone (3%) corresponds to the coastal shoreline, with a very high vulnerability owing to shallow groundwater within highly permeable sandy sediments (Boufekane et al., 2019).

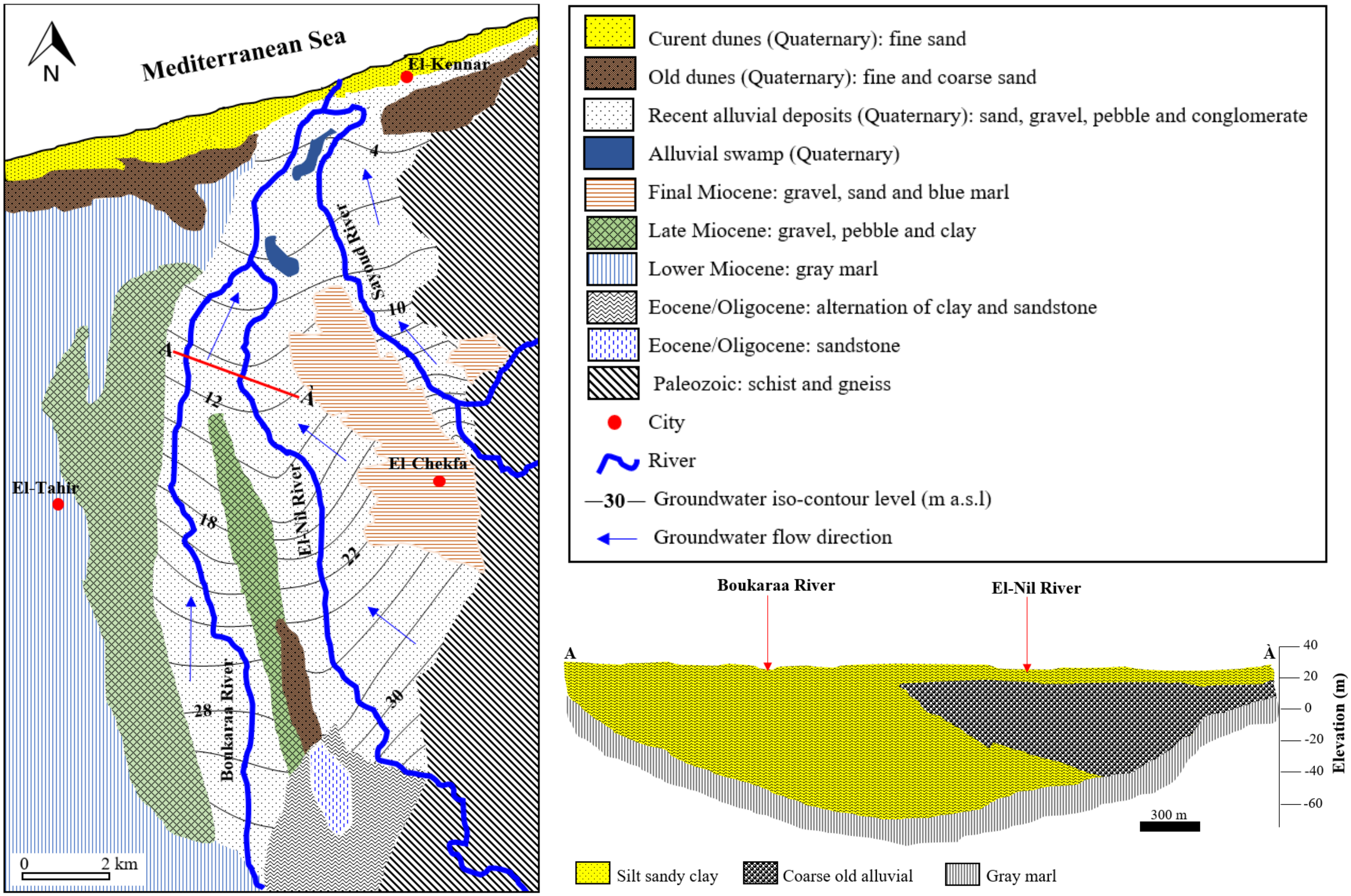

Fig. 2. Surface geological deposits of the Plain of El-Nil River (Durozoy, 1954), and cross-section (A-À) conducted in the study area by CGG (1971). Groundwater iso-contour levels and groundwater flow direction are from the present study.

3 Material and methods

3.1 Sampling and laboratory analyses

3.1.1 Sampling network and protocol

For the present study, a comprehensive water sampling campaign and piezometric measurements were conducted on November 12−14, 2021. The water sampling program included 27 groundwater samples spatially distributed over the entire study area, seven surface water samples collected from the rivers crossing the study area, and one water sample collected from the Mediterranean Sea (Fig. 1). Groundwater samples were collected from shallow irrigation wells, featuring a groundwater depth ranging from 3 to 6 m below the ground surface, during irrigation of agricultural fields. Surface water samples were collected directly from each river using 100-mL luer-lock syringe samplers. During the groundwater and surface water sampling process, physico-chemical parameters (temperature, pH, EC, total dissolved solid (TDS)) were measured *in-situ* using a calibrated multiparameter probe (HI-9829, Hanna Instruments©). The water collected for major anion and cation analyses was filtered *in-situ* using 0.45-μm nitrocellulose membrane filters attached to 100-mL luer-lock syringe samplers, before being poured in two separate 40-mL amber glass bottles. The bottle for cation analysis was acidified to pH <2 by adding 2-3 drops of ultrapure nitric acid (HNO_3) to prevent major cation precipitation or adsorption during storage. Water samples for anion analyses were collected in a similar way but were not acidified. The water for δ^2H_{H2O} and $\delta^{18}O_{H2O}$ analyses was collected in one 40-mL amber glass bottle, whereas filtered water for $\delta^{15}N_{NO3}$ and $\delta^{18}O_{NO3}$ analyses was collected in 50-mL polyethylene bottles. All samples were collected in bottles without headspace; furthermore, these bottles were equipped with caps containing Teflon septa parafilm to prevent evaporation. During fieldwork, all water samples were temporarily stored in a portable cooler before being transferred to a refrigerator for storage at 4°C at the completion of the fieldwork-day until analysis. The samples collected for isotopic analysis of nitrate were the exception; they were stored frozen to avoid variations caused by biological processes until the targeted isotopic analyses were performed in the laboratory.

3.1.2 Chemical and stable isotope analyses

Major cations and anions (HCO_3^-, Br^-, NO_3^-, Cl^-, K^+, Mg^{2+}, NH_4^+, Na^+, Ca^{2+} and SO_4^{2-}) were analyzed at the Laboratory of the Hydrogeology Department of the University of Corsica (France). HCO_3 concentrations were determined by volumetric titration to pH 4.5 using a digital titrator HACH (Hach Company©, Loveland, CO, USA). The other anion and cation concentrations were determined using a Dionex ICS 1100 ion chromatograph (Thermo Fischer Scientific, Waltham, USA), where the validity of the analytical results were confirmed by testing the ionic balance, for which a value of ±10% was considered acceptable (Hounslow, 1995). The δ^2H_{H2O} and $\delta^{18}O_{H2O}$ measurements were performed at the Laboratory of the Institute of Soil Physics and Rural Water Management in Vienna (Austria). These isotopic values were determined using a laser-based isotope analyzer (Picarro L2130-*i*) according to the analytical scheme recommended by the International Atomic Energy Agency (IAEA) (Penna et al., 2010). Nitrate isotopic composition ($\delta^{15}N_{NO3}$ and $\delta^{18}O_{NO3}$) was analyzed at the Helmholtz Center for Environmental Research in Halle/Saale (Germany), using the denitrifier method with bacteria strains of *Pseudomonas chlororaphis* (ATCC #13985 equal to DSM-6698) according to the protocols recommended by Casciotti et al. (2002) and Sigman et al. (2001). The isotope values, expressed in permil (‰) using delta (δ) notation, were calculated using Equation 1, where R_{sample} and R_{standard} are the sample and the international reference standard ratios of the heavier to the lighter isotope, respectively (i.e., $^{2}H/^{1}H$, $^{15}N/^{14}N$, or $^{18}O/^{16}O$).

$$\delta = \frac{R_{sample} - R_{standard}}{R_{standard}} \quad (1)$$

The international reference standards relative to which the sample isotopic values are reported as Vienna Mean Standard Ocean Water (VSMOW) for $\delta^{2}H_{H2O}$ and $\delta^{18}O_{H2O}$ and $\delta^{18}O_{NO3}$, and atmospheric nitrogen (AIR) for $\delta^{15}N_{NO3}$. The precision of the analytical instrument was generally better than ±0.5‰ for $\delta^{2}H_{H2O}$ and ±0.1‰ for $\delta^{18}O_{H2O}$; whereas the reproducibility for the $\delta^{15}N_{NO3}$ and the $\delta^{18}O_{NO3}$ measurements were ±0.6‰ and ±0.4‰, respectively.

3.2 Seawater intrusion assessment

Seawater intrusion influence was assessed by using a hydrochemical facies evolution diagram (HFE-D) (Giménez-Forcada and Sánchez San Román, 2015). This approach has successfully been applied for assessing seawater intrusion influence in several Mediterranean coastal aquifers (e.g., Giménez-Forcada, 2019; El-Kholy et al., 2022; Najib et al., 2017; Boumaiza et al., 2020). The HFE-D provides a straightforward approach for distinguishing freshwater and saltwater types, as well as the gradual evolutive intermediate sub-stages between these two water types. The HFE-D considers the concentrations of major anions (HCO_3, SO_4, Cl, and NO_3) and cations (Ca, Mg, Na, and K) of water samples, as well as those of a saltwater reference (i.e., Mediterranean Sea). For the HFE-D diagram, a conservative mixing line (CML) can be established to separate the water samples belonging to the freshening phase from those subject to seawater intrusion. The freshening phase includes the gradual evolutive freshening sub-stages f_1, f_2, f_3, and f_4 before distinguishing the freshwater (FW); the water samples falling on freshening sub-stages and freshwater correspond to water unaffected by seawater intrusion. The seawater intrusion phase considers the gradual evolutive sub-stages i_1, i_2, i_3, and i_4 preceding the saltwater condition (SW); the water samples falling on seawater intrusion sub-stages and saltwater correspond to water affected by seawater intrusion. Water samples that plot in the center of the HFE-D can belong to either the freshening or seawater intrusion trends, depending on their position relative to the CML and also their determined water type (Giménez-Forcada and Sánchez San Román, 2015).

3.3 Identifying nitrate sources and estimating their apportionments

To assess nitrate sources in water samples, the $\delta^{15}N_{NO3}$ versus $\delta^{18}O_{NO3}$ diagram (Kendall, 1998) was used. This diagram shows individual fields corresponding to specific sources of nitrate. These sources include atmospheric precipitation (AP), NO_3-based fertilizers (NOF), sewage and manure (S&M), NO_3-based desert deposit (DD), NO_3 that is formed from nitrification of NH_4-fertilizers (NHF) or soil organic nitrogen (SON). Furthermore, the logarithmic diagram of NO_3/Cl versus Cl (Torres-Martínez et al., 2021) was used to support outcomes from the $\delta^{15}N_{NO3}$ versus $\delta^{18}O_{NO3}$ diagram, whereas the MixSIAR model (Parnell et al., 2010) was used to estimate the proportional contribution of the different nitrate sources in the water systems (Cao et al., 2021; He et al., 2022; Torres-Martínez et al., 2021). More detail on the MixSIAR model development can be found in Stock et al. (2018). The main inputs in the MixSIAR model are the values of $\delta^{15}N_{NO3}$ and $\delta^{18}O_{NO3}$ measured in water samples and the different end-member isotopic values of the sources of nitrate. Here, the end-member isotopic values of atmospheric precipitation, NO_3-based fertilizers, nitrification of NH_4-fertilizers, soil organic nitrogen and sewage/manure were considered, whereas NO_3-based desert deposits were excluded as the study area is in the Mediterranean region with minimal effect of desert deposition. Due to the limited number of samples analyzed for nitrate isotopic composition (n = 21), the end-member isotopic value ranges of the five considered sources of nitrate were adopted from Torres-Martínez et al. (2021a), who investigated nitrate contamination in an area with comparable anthropogenic nitrate sources. The $\delta^{15}N_{NO3}$ values assigned to possible end-members values are 0.11±1.69‰ for atmospheric precipitation, −0.07±2.85‰ for NO_3-based fertilizers, 1.24±1.44‰ for NH_4-fertilizers, 3.26±1.99‰ for soil organic nitrogen, and 10.14±4.53‰ for sewage and manure; the $\delta^{18}O_{NO3}$ values are 54.97±7.63‰ for atmospheric precipitation, 24.12±3.17‰ for NO_3-based fertilizers, 3.44±2.47‰ for NH_4-fertilizers, 3.34±2.04‰ for soil organic nitrogen, and 5.69±2.91‰ for sewage and manure.

4 Results and discussions

4.1 Seawater intrusion

4.1.1 Isotopic evidence of water origin and salinization

The δ^2H and $\delta^{18}O$ values for the samples from groundwater, rivers, and the Mediterranean Sea are listed in the Supplemental Table S1 and shown in Fig. 3. The surface water samples collected from the rivers revealed $\delta^{18}O_{H2O}$ values ranging from −6.91‰ to −6.22‰ with a median value of −6.76‰, and δ^2H_{H2O} values ranging from −45.2‰ to −36.6‰ with a median value of −40.7‰. The collected water sample from the Mediterranean Sea displays enriched isotopic values, with −1.07‰ for $\delta^{18}O_{H2O}$ and 6.2‰ for δ^2H_{H2O}. The $\delta^{18}O_{H2O}$ and δ^2H_{H2O} values are interpreted according to the Global Meteoric Water Line (GMWL) (Craig, 1961) and the Western Mediterranean Meteoric Water Line (WMMWL) (Celle, 2000). In Fig. 3, the surface water samples display relatively depleted isotopic signatures compared to the groundwater suggesting water origination from higher altitudes within the surrounding mountains, from which the rivers took source. The surface water samples collected from the El-Nil River (#3 and #4), Boukaraa River (#5 and #6), and Sayoud River (#7) plot on/near the WMMWL (Fig. 3), suggesting limited isotopic fractionation effects beyond those directly associated with the precipitation process. In fact, these surface water samples have d-excess values ranging from +13 to +15.7‰, which are comparable to that of the WMMWL (14‰). Conversely, surface water sample #1 (collected from the downstream portion of the El-Nil River) and surface water sample #2 (collected from the Tassift River) deviate from the WMMWL, suggesting that evaporation or/and mixing processes affect these surface waters. More specifically, sample #2 from the Tassift River plots below the WMMWL and exhibits a relatively low d-excess value (10.08‰) suggesting that this surface water is potentially experiencing evaporation that decreased its d-excess. In fact, the Tassift River contains an open 0.3 km^2-surface water body (Fig. 1) where evaporation is likely occurring. Nonetheless, because sample #2 also plots on the GMWL, it is equally possible that Tassift River water is also influenced by mixing with another water such as local precipitation. Water sample #1 from the lower El-Nil River (Fig. 1) plots below the WMMWL but above the GMWL (Fig. 3) suggesting dominance of mixing process over evaporation; the mixing process is supported by its d-excess value of +11.52‰. Such a mixed origin of sample #1, which was collected downstream of the confluence of the Sayoud, Boukaraa, and Tassift Rivers with the El-Nil River (Fig. 1) is consistent with mixing of the surface water from the upstream of the El-Nil River (sample #3), the Sayoud River (#7) and the Tassift River (#2), explaining its intermediate isotopic plot on Fig. 3.

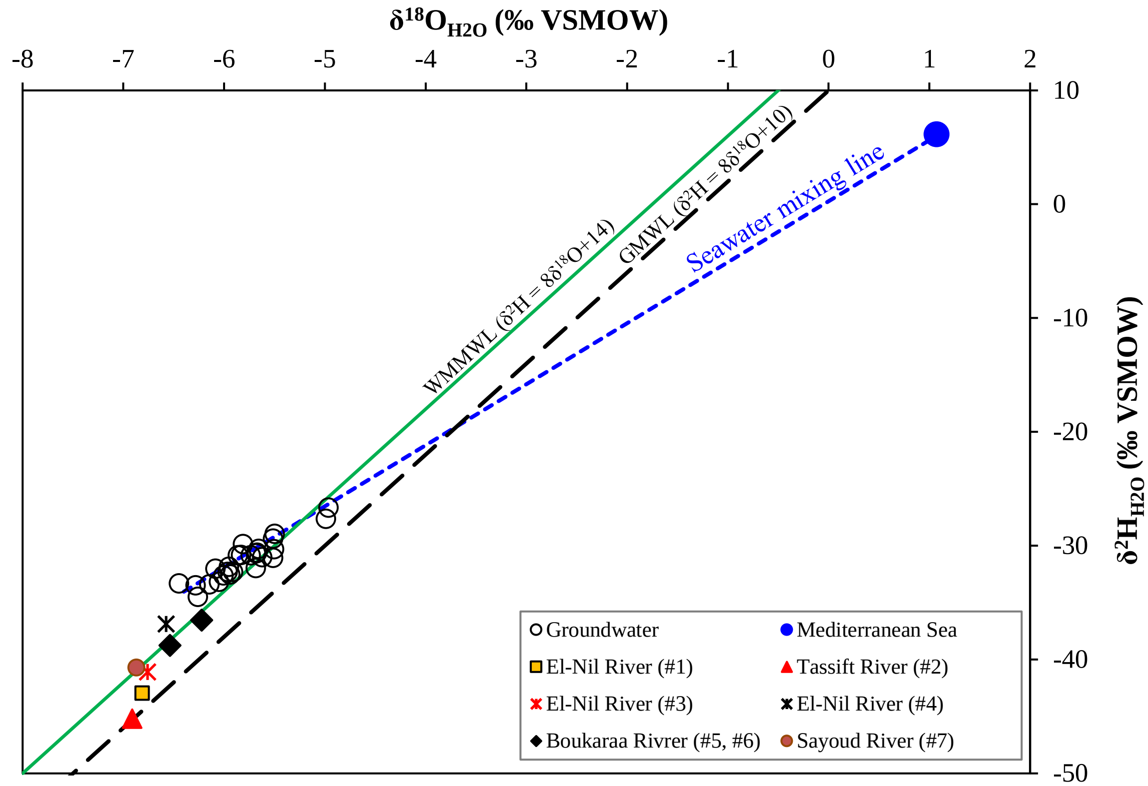

Fig. 3. Distribution of isotopic values of the collected water samples. Seawater mixing line is the line linking the groundwater samples to the Mediterranean Sea sample. The GMWL is from Craig (1961), while the WMMWL is from Celle (2000).

The isotopic values of groundwater range from −6.45‰ to −4.96‰ with a median value of −5.81‰ for $\delta^{18}O_{H2O}$; and from −34.5‰ to −26.6‰ with a median value of −31‰ for $\delta^{2}H_{H2O}$. These groundwater isotopic signatures are comparable with other North-Africa Mediterranean coastal aquifers (Boumaiza et al., 2020; Chafouq et al., 2018; Elmeknassi et al., 2022) and present a typical range found along the fresh- to seawater continuum (Erostate et al., 2018). In Fig. 3, groundwater samples center around the WMMWL suggesting that groundwater in the study area is recharged through direct infiltration of rainwater with minimal evaporation effect. This observation corresponds to what could be expected for the unconfined aquifer in the study area, which is composed of granular material with hydraulic conductivities between 2.32×10^{-3} and 3.58×10^{-3} m/s (Boufekane, 2017). The range of negative isotopic values of groundwater are comparable to those of Mediterranean precipitation that occurs during the wet season ($\delta^{18}O_{H2O}$ from −5.01 to −2.84‰, and $\delta^{2}H_{H2O}$ from −28.1 to −17.1‰) (IAEA, 2021), suggesting that local groundwater is chiefly recharged during the wet season. Recharge during the wet season is expected for study areas with sub-humid climate conditions that are dominated by increased winter precipitation relative to dry summers. The groundwater d-excess values from +12.30 to +18.26‰ (Supplemental Table S1) are indicative of modern recharge, whereas the calculated d-excess median value of 15.06‰ is typical for recharge derived from Mediterranean moisture sources (Celle-Jeanton et al., 2001; Gat and Carmi, 1970).

Fig. 3 shows a clear indication of groundwater heavy isotope enrichment toward the Mediterranean Sea sample (blue point in Fig. 3) along a mixing line with seawater, indicating some mixing of local groundwater with Mediterranean seawater. Chloride concentrations in river water (median = 60 mg/L) are lower than those of groundwater (median = 80 mg/L), suggesting a soil water influence during surface flow and/or infiltration (Appelo and Postma, 2005). Moreover, the combination of groundwater-Cl with $\delta^{18}O_{H2O}$ values (Supplemental Fig. S1) shows a slight positive correlation suggesting an increase in salinity accompanying heavy isotope enrichment. The positive relationship between Cl and $\delta^{18}O_{H2O}$ suggests a possible evaporative influence and/or groundwater mixing with seawater (Elmeknassi et al., 2022). Here, the evaporation effect can result from the infiltration of irrigation water-return flow, as the study area includes substantial agricultural activities characterised by potential recharge contribution of about 60 mm/year from irrigation (Boufekane, 2017). However, the evaporation effect does not appear to be very pronounced based on isotopic data (Fig. 3).

4.1.2 Evaluating and delineating seawater intrusion influence

Fig. 4 shows the distribution of the collected groundwater/surface water samples within the HFE-D; the water samples impacted by seawater intrusion are underlined in red, whereas samples characterised as belonging to the freshwater type are underlined in green. Seventeen of the total analysed groundwater samples (27) were identified in the freshening stage, or as freshwater (unaffected by seawater), whereas 10 samples were identified in seawater intrusion stage or as saltwater (affected by seawater intrusion). Unaffected groundwater samples include two samples (#22 and #34) identified in the freshening sub-stage f_2 corresponding to the Na-MixCl facies; three samples (#11, #30 and #33) in the freshening sub-stage f_3 corresponding to the Na-MixHCO$_3$ or MixNa-MixHCO$_3$ facies; four samples (#19, #23, #24, and #26) in the freshening sub-stage f_4 corresponding to the MixCa-HCO$_3$ or MixNa-HCO$_3$ facies; and eight samples (#9, #10, #21, #25, #27, #28, #29, and #32) identified as freshwater corresponding to the Ca-HCO$_3$ facies. The ten affected groundwater samples by seawater include eight samples (#8, #12, #13, #14, #17, #18, #20, and #31) identified in the sub-stage i_1 of seawater intrusion with MixCa-MixHCO$_3$ or Ca-MixHCO$_3$ facies; one sample (#16) located in the sub-stage i_3 of seawater intrusion corresponding to MixNa-Cl facies; and one sample (#15) with Na-Cl facies corresponding to saltwater in HFE-D (Fig. 4). Regarding the seven analysed surface water samples, five samples (#3, #4, #5, #6 and #7) were identified as freshwater corresponding to Ca-HCO$_3$ facies, whereas two samples (#1 and #2) were identified as affected by seawater but in the sub-stage i_1 of seawater intrusion corresponding to MixCa-MixHCO$_3$ facies.

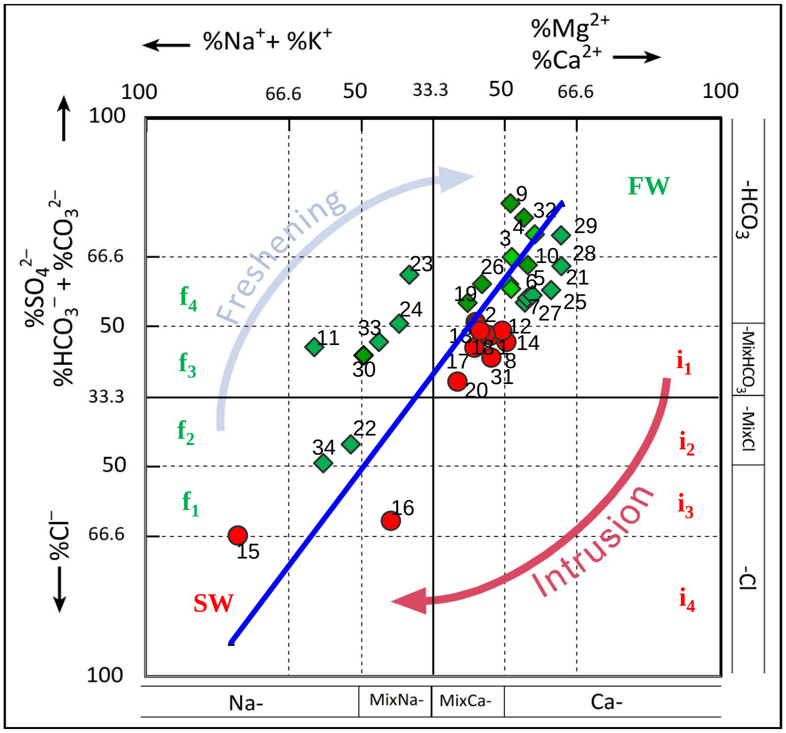

Fig. 4. HFE-D results for the collected water samples considering their position in relation to the intrusion and freshening sub-stages.

Fig. 5 shows the spatial distribution of unaffected/affected water samples by seawater intrusion according to the HFE-D. As expected, the area affected by the seawater intrusion is in the northern part of the study area next to the Mediterranean Sea. The affected area includes surface water samples #1 and #2 collected from downstream reaches of the El-Nil River and the Tassift River, respectively. Both sample #1 and #2 are located relatively close to the Mediterranean Sea, suggesting possible direct influence of the Mediterranean Sea through a diffusion mechanism supported by a Cl concentration gradient. When the Sea is turbulent, the diffusion process could be simultaneously supported with an advective transport and seawater aerosol (Ceburnis et al., 2014; Freney et al., 2021). Surface seawater influence on sample #1 appears reasonable as this sample was collected only 0.5 km from the Mediterranean Sea. The affected surface water sample #2 is, however, located 2.8 km far from the Mediterranean Sea along the river. Surface water sample #3 is located near surface water sample #2 at similar distance from the Mediterranean Sea (Fig. 5). Nonetheless, sample #3 is identified as unaffected by seawater intrusion. Sample #3 was collected just downstream of the confluence of the El-Nil River and Boukaraa River. Each of these rivers is dominated by the Ca-HCO_3 facies (see in Fig. 5 the chemical facies of samples #4, #5 and #6 collected from the El-Nil River and Boukaraa Rivers). The surface elevation of the study area decreases from average altitude of about 47 m a.s.l. in the upper reaches of both the El-Nil and Boukaraa Rivers to an average of 8 m a.s.l. at the confluences of these river near the location of the sample #3. The physiography leads to high surface water discharge (high streamflow) of Ca-HCO_3-rich waters, and thus limits surface seawater progression at the location of the sample #3; reason for which sample #3 is of Ca-HCO_3 composition. The Tassift River (i.e., sample #2) drains a small local watershed (Bouakkaz and Zentout, 2020), and contains a 0.3 km^2-surface water body located upstream of where sample #2 was collected (Fig. 5). These features involve low streamflow through the Tassift River, offering consequently a possible saltwater advancing from Mediterranean Sea; potential reason for which sample #2 is identified as affected by seawater. Here, the seawater influence —particularly at the sampling point #2— was maybe combined with evaporation effect evidenced from the stable water isotope signatures (Fig. 3). The open 0.3 km^2-surface water body through which the Tassift River flows likely contains evapo-concentrated water that can contribute to downstream salinity (samples #1 and #2).

The affected surface water samples #1 and #2, with facies MixCa-MixHCO_3 according to HFE-D, are surrounded by affected groundwater samples (#8, #14, #17, #18 and #20) corresponding to the same facies (Fig. 5). Considering the similarity in water facies, this suggests possible interactions between the surface waters and groundwater. The affected surface water samples #1 and #2 have lower Cl concentration relative to the affected surrounding groundwater samples, suggesting possible Cl diffusion from high Cl-concentrated groundwater to the less Cl-concentrated surface water driven by the concentration gradient. Such interactions could contribute to more mixing processes as evidenced through the Gibbs diagram (Gibbs, 1970) (Fig. 6a), showing that samples #1 and #2 tend towards more mixing influence compared to the other surface water samples from the study area. Furthermore, Piper's diagram (Piper, 1944) (Fig. 6b) shows that all the surface water samples are Ca-HCO_3 water type, indicative of recent meteoric precipitation without mixing and/or indicative of carbonate dissolution influence (Drouiche et al., 2022), except the two samples #1 and #2 plotting within the mixing zone bordering the zone of Ca-HCO_3 water type. This agrees with MixCa-MixHCO_3 corresponding to early sub-stage i_1 of seawater influence according to HFE-D.

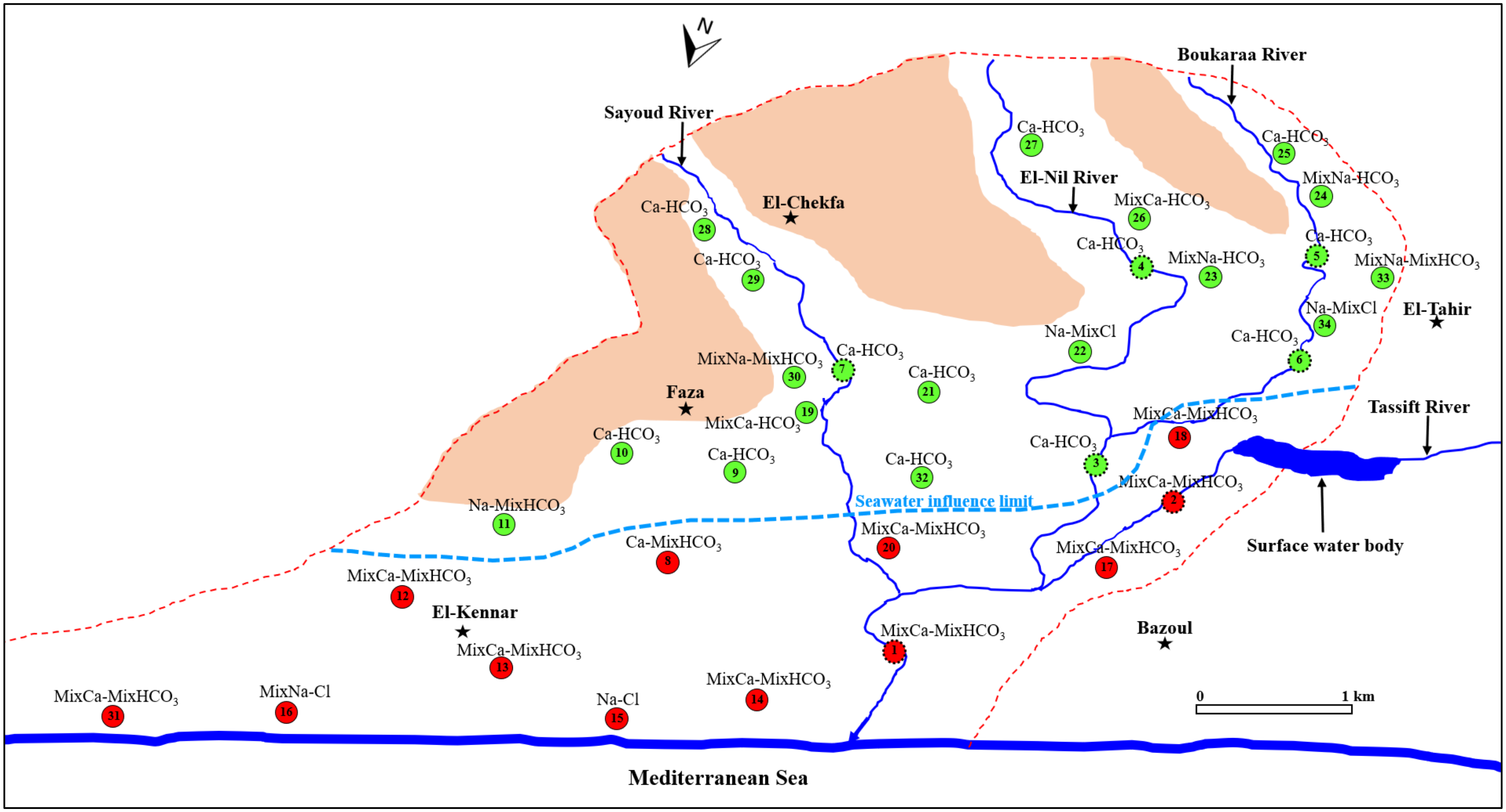

11 water sample unaffected by seawater 13 water sample affected by seawater surface water sample

MixCa-MixHCO$_3$: determined chemical facies according to HFE-D

Hills without agricultural activities

Fig. 5. Spatial distribution of water samples unaffected/affected by seawater intrusion according to HFE-D.

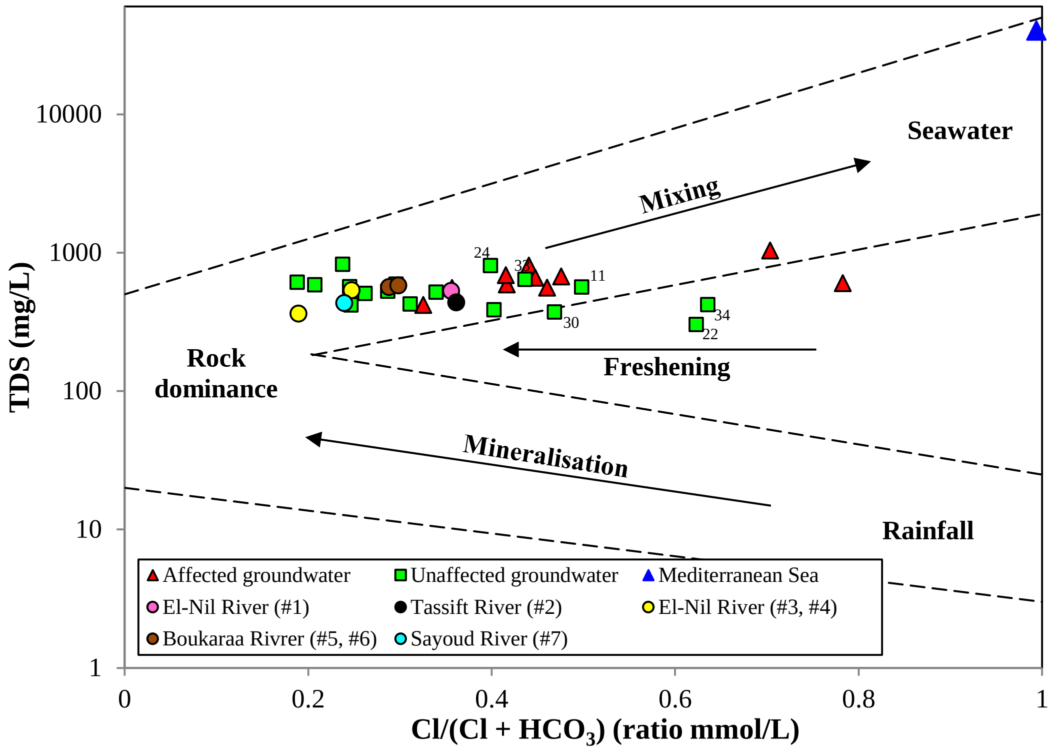

(a)

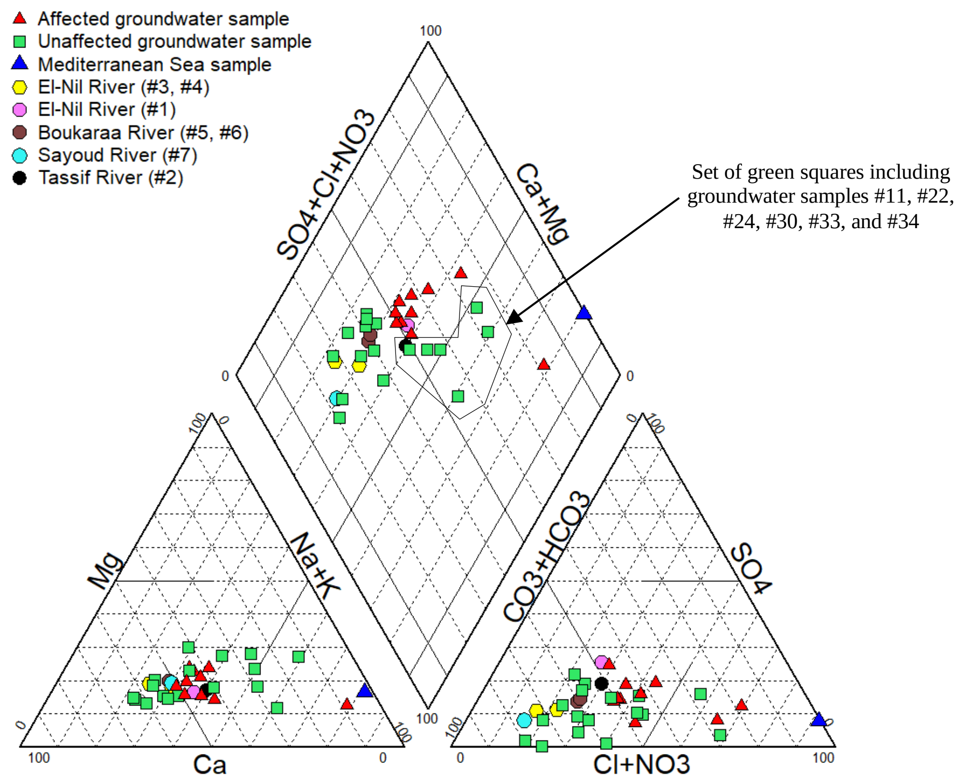

(b)

Fig. 6. Plot of the collected water samples on (a) Gibbs's diagram and (b) Piper's diagram.

Groundwater affected by seawater intrusion includes samples #8, #12, #13, #14, #15, #16, #17, #18, #20, and #31 (Fig. 5). Hence, seawater intrusion largely impacts the northern part of the study area, despite the facts that: (i) groundwater exploitation for agricultural activities occurs over the majority of the study area, and (ii) most municipal wells are located in the southern part of the study area (Amiour, 2015). Seawater intrusion is chiefly limited to the northern region that is characterised by relatively flat terrain (slopes $\leq 0.2\%$), and does not advance further south where the terrain exhibits an average slope of 7%. The piezometric map (Fig. 2) demonstrates that the southern area exhibits a steeper hydraulic gradient (0.004) compared to the northern area (0.001). Therefore, the physiography of the study area and its effect on hydraulic gradients appears to be the main factors controlling the inland progression of seawater intrusion. Hence, high groundwater flow rates toward the Mediterranean Sea from the southern part of the study area limits inland seawater intrusion.

At the inland limit of seawater intrusion, the unaffected groundwaters are dominated by the Ca-HCO_3 water type (samples #9, #10, and #32; Fig. 5). Similarly, the unaffected groundwaters collected from the southern border of the study area are also characterized as Ca-HCO_3 type waters (samples #25, #27, #28, and #29 in Fig. 5). These Ca-HCO_3 type waters correspond to meteoric precipitation that recharges the aquifer in the southern part of the study area, which is further supported by the wells sampled in the south exhibiting the highest groundwater levels (Fig. 2). Thus, the HFE-D plot indicates that all groundwaters south of the seawater intrusion limit are unaffected by mixing with seawater (Fig. 5). Nevertheless, in addition to the Ca-HCO_3 type waters, mixed water types were identified from this region (Fig. 5). Those groundwater samples exhibiting characteristics of being mixed water types includes groundwater samples #26 and #19 that are classified as MixCa-HCO_3 water type (Fig. 5). These groundwaters appear to be experiencing a freshening process by mixing with dilute Ca-HCO_3 type waters. Other mixed water types within the seawater unaffected groundwater samples include sample #11, which is a Na-MixHCO_3 type water, samples #30 and #33, which are MixNa-MixHCO_3 type waters, and samples #23 and #24, which belong to MixNa-HCO_3 type waters (Figs. 4, 5). All of these groundwaters appear to have evolved from waters with relatively high Na concentrations that have since be subjected a freshening process via mixing with dilute Ca-HCO_3 type waters. This scenario is consistent with the fact that these groundwaters all plot in the advanced freshening sub-stages f_3 and f_4 of the HFE-D (Fig. 4). Conversely, the two groundwater samples #22 and #34, which are classified as Na-MixCl mixed type waters within the seawater unaffected groundwater samples, plot in the early freshening sub-stage f_1 on the HFE-D, suggesting the potential evolution from an initial saline water that is now undergoing freshening. The freshening process of groundwater samples #11, #22, #24, #30, #33, #34 is also apparent on the Gibbs's diagram (Fig. 6a) showing that the majority of these groundwater samples plot along the freshening trend. The plotting of these groundwater on Piper's diagram (Fig. 6b) illustrates that samples #24, #30, and #33 are mixed water type dominated by Na and HCO_3, which also agrees with the HFE-D results (Fig. 4). In contrast, groundwater samples #11, #22, and #34 plot as Na-Cl type waters on the Piper diagram, which also agrees with the HFE-D result (Fig. 4, 6b). Together these data indicate that groundwater from the study region evolves from Ca-HCO_3 type waters in the south to more Na-rich waters in the north. This pattern of changing groundwater composition is consistent with the notion that cation-exchange of Ca for Na on clay minerals can explain the increase of Na concentrations in the Plain of the El-Nil River groundwaters (Appelo and Postma, 2005). However, the change of water chemistry along areas neighbouring urban sectors also suggests that Na in underlying groundwaters could also reflect the presence of anthropogenic sources such as wastewater discharge (Erostate et al., 2018; Zendehbad et al., 2019).

4.2 Sources and apportionment of nitrate in water systems

NO_3 concentrations in groundwater from the Plain of the El-Nil River range from 0.38 to 75 mg/L. Only two of the 27 collected groundwater samples (i.e., #20 and #34) have NO_3 concentrations exceeding the drinking water limit of 50 mg/L (WHO, 2017). However, 67% of the groundwater samples reveal NO_3 concentrations exceeding the natural baseline threshold value of 5 mg/L (Appelo and Postma, 2005; Panno et al., 2006), suggesting anthropogenic impact over the study area. Fig. 7 shows that three specific areas of anthropogenic influence can be distinguished based on NO_3 concentrations >5 mg/L. These groundwaters are from: (i) the northeastern region of the study area around El-Kennar village; (ii) the region ranging from El-Chekfa village to Bazoul village passing by the border of Faza village; and (iii) the western-central region from El-Tahir City to Bazoul village (the three areas are indicated with dashed red lines in Fig. 7). Groundwater samples with NO_3 concentrations <5 mg/L are chiefly between El-Kennar village and Faza/Bazoul villages in northern part of the study area, and from central to southwestern part of the study area (Fig. 7). The present study reveals that the highest NO_3 concentrations (i.e., 60 mg/L $\leq NO_3 \leq$ 75 mg/L) occur in wells #20 and #34, which are located close to the Boukaraa River and the El-Nil River (Fig. 7). These elevated NO_3 concentrations are likely not related to contributions from surface water, at least during the sampling campaign of the present study, because the NO_3 concentration in water samples from these rivers were lower than in the groundwater. Considering all the study area, it is probable that continuous sources of nitrate are affecting the study area because the maximum NO_3 concentration of 75 mg/L from the present study is comparable to the maximum of 90 mg/L observed in 2014 (Amiour, 2015).

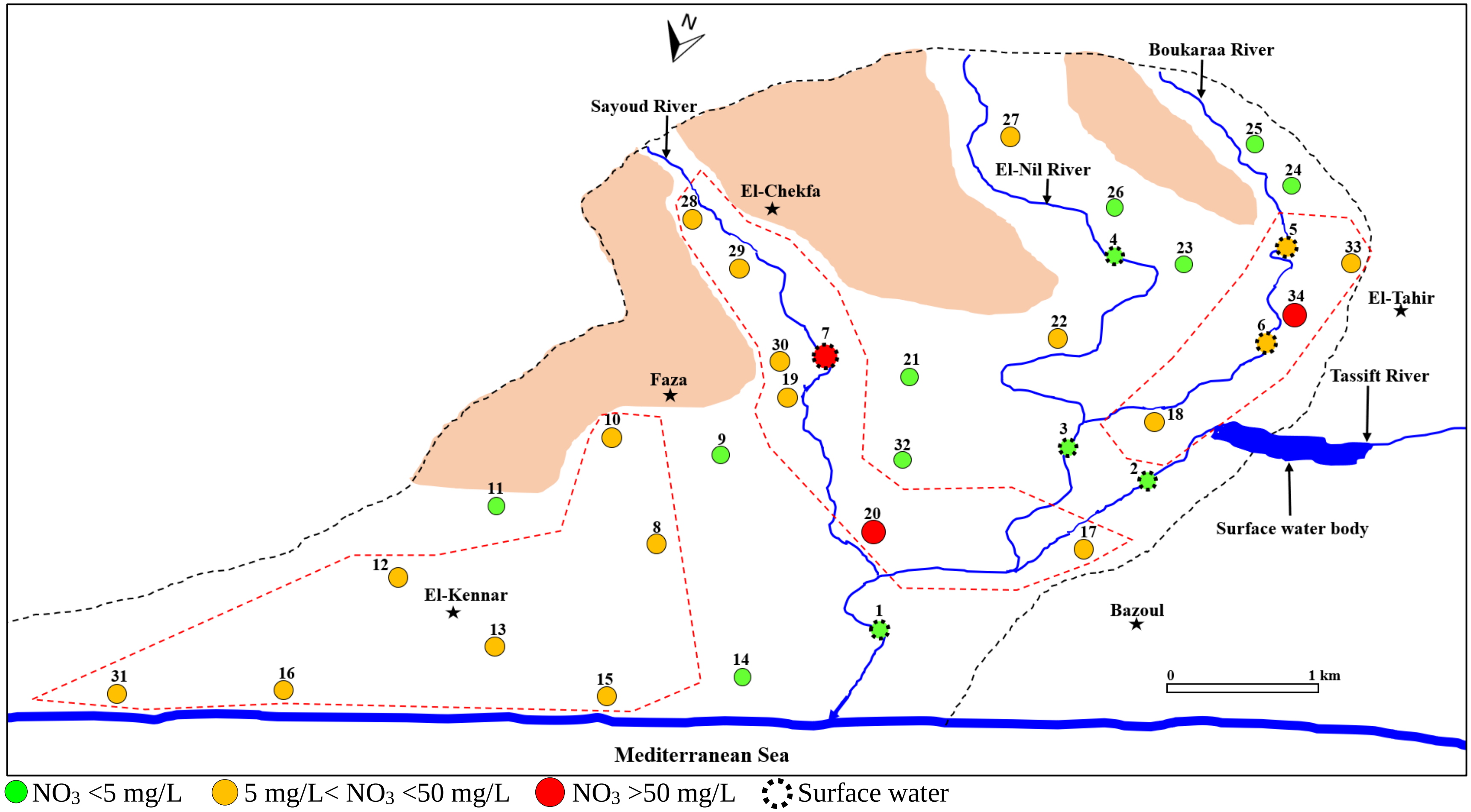

Fig. 7. Spatial distribution of NO_3 concentrations over the study area. In dashed red are the main sectors revealing anthropogenic nitrate influence.

Groundwater from the study area exhibits $\delta^{15}N_{NO3}$ values ranging from +0.9‰ to +23.8‰, with a median value of +10.1‰, and $\delta^{18}O_{NO3}$ values varying between +5.3‰ and +21.5‰, with a median value of +11.9‰. Surface water samples from the study area have $\delta^{15}N_{NO3}$ values ranging from −1.0‰ to +15.3‰, with a median value of +10.4‰, and $\delta^{18}O_{NO3}$ values from +6.5‰ to +16.2‰, with a median value of +9.6‰. On the $\delta^{15}N_{NO3}$ versus $\delta^{18}O_{NO3}$ diagram, all groundwater samples show $\delta^{15}N_{NO3}$ and $\delta^{18}O_{NO3}$ compositions that are consistent with those of manure and sewage (Fig. 8a). Six groundwater samples (#10, #13, #17, #23, #27 and #32) plot in the zone where manure and sewage overlap with (i) NO_3 from soil-derived nitrogen and (ii) NO_3 from nitrification of NH_4 in fertilisers. The combined analysis of $\delta^{15}N_{NO3}$ and $\delta^{18}O_{NO3}$ also makes it possible to evaluate nitrate transformation processes in a water system subjected to microbial denitrification because $\delta^{15}N_{NO3}$ and $\delta^{18}O_{NO3}$ ratios increase in a predictable fashion during denitrification while NO_3 concentrations decrease (Böttcher et al., 1990; Wassenaar, 1995). Denitrification in water systems is commonly reflected by positive 2:1 correlation between $\delta^{15}N_{NO3}$ and $\delta^{18}O_{NO3}$ (Mengis et al., 1999; Singleton et al., 2007). The scattered distribution of our $\delta^{15}N_{NO3}$ and $\delta^{18}O_{NO3}$ data (Fig. 8a) makes it difficult to distinguish between mixing of differently denitrified sources and actual denitrification.

Plotting the chemical results of the groundwater and surface water samples on the diagram of NO_3/Cl versus Cl (Torres-Martínez et al., 2021) shows that most of these water samples fall in the sewage input zone (Fig. 8b); this indicates that wastewater contributes substantial NO_3 to studied water systems. However, some groundwater samples also indicate trends toward the manure inputs zone on the NO_3/Cl versus Cl diagram (Fig. 8b) suggesting that inputs from manure also potentially influence the NO_3 pools in the studied waters. Results of the MixSIAR model revealed that sewage and manure (S&M) are the main nitrate sources in groundwater (48.8%) and surface water (40.5%), which is consistent with the $\delta^{15}N_{NO3}$ versus $\delta^{18}O_{NO3}$ diagram and the of NO_3/Cl versus Cl diagram (Fig. 8a, b). The other sources of nitrate considered by the model exhibit the same relative proportional order and with comparable contributions in groundwater (soil organic nitrogen=17.5%, NO_3-based fertilizers=13.8%, atmospheric precipitation=11.4%, NH_4-fertilizers=8.5%; Fig. 8c) and surface water (soil organic nitrogen=20.6%, NO_3-based fertilizers=18.4%, atmospheric precipitation=12.2%, NH_4-fertilizers=8.3%; Fig. 8d). These results suggest that anthropogenic activities have an important influence on NO_3 concentrations rather than NO_3 source apportionments between groundwater and surface water (Li et al., 2022).

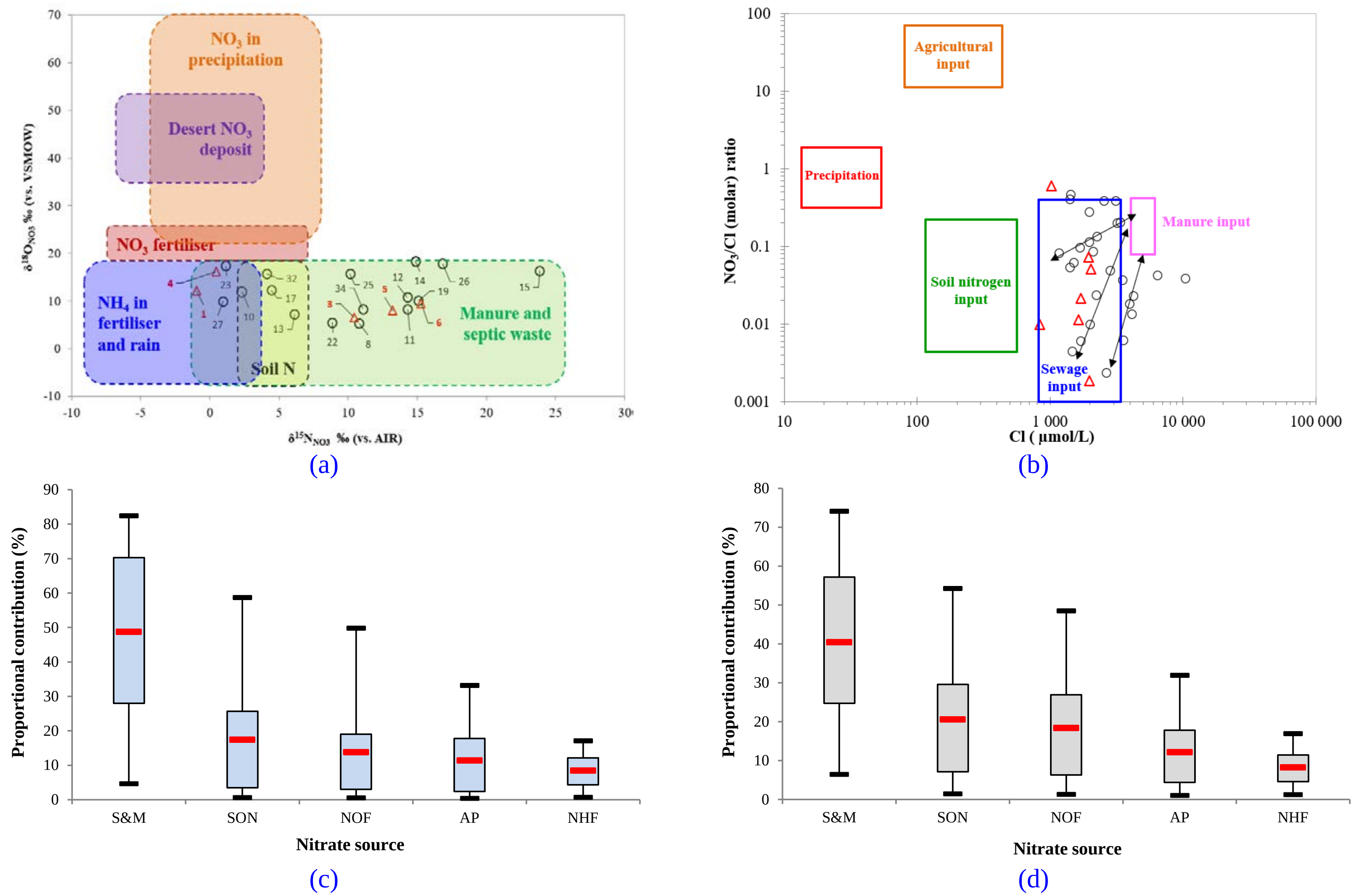

Fig. 8. (a) Plot of $\delta^{15}N_{NO3}$ versus $\delta^{18}O_{NO3}$ values (Kendall, 1998) where black circle indicates groundwater sample and red triangle displays surface water sample; (b) Plot of Cl molar concentrations versus NO_3/Cl molar ratios (Torres-Martínez et al., 2021) where black arrows suggest potential mixing between sewage and manure inputs; (c) apportionment of nitrate sources in groundwater based on MixSIAR; and (d) apportionment of nitrate sources in surface water based on MixSIAR. In (c) and (d), S&M: sewage and manure, SON: soil organic nitrogen, NOF: NO_3-based fertilizers, AP: atmospheric precipitation, NHF: NH_4-fertilizers. Boxplots illustrate the 25th, 50th, and 75th percentiles, while the whiskers indicate 5th and 95th percentiles.

The study area is a traditional agricultural plain that has been cultivated, irrigated, and mostly fertilized by animal manure for several decades; such practices result in the accumulation of soil organic nitrogen and NO_3-based fertilizers in the soils and shallow groundwaters (He et al., 2022), which can explain their relative proportions detected within the study area from the present study. However, the three approaches (i.e., $\delta^{15}N_{NO3}$ versus $\delta^{18}O_{NO3}$ diagram, NO_3/Cl versus Cl diagram, and MixSIAR model) used to distinguish the nitrate sources indicate that synthetic fertilizers were not the main source of nitrate in local groundwater and surface water systems. It is surprising that sewage and manure constitute the main sources of nitrate as the previous studies undertaken on the study area suggested the extensive use of synthetic fertilizers as the primary source of nitrate to local groundwaters (Amiour, 2015; Boufekane, 2017). However, these researchers did not consider that possible influence of sewage and manure to the nitrate pool. Based on the finding of the present study, nitrate derived from sewage sources can be explained by wastewater discharge/leakage from the inadequate private sanitation systems, which are constructed with open-bottoms through human waste can directly seep into the subsurface and reach groundwater. These private sanitation systems are still common in the region where segments of the local population cannot connect with the municipal sewage system. In addition, nitrate derived from sewage also likely results from wastewater discharge of the local sanitation networks. Specifically, wastewater sanitation networks of the neighboring urban communities drain directly into the rivers within the study area, without prior treatment (Boumaiza et al., 2021). Together, these sources can explain why surface water samples #1, #3, #4, #5 and #6 collected from the El-Nil and Boukaraa rivers revealed N isotope signatures that are characteristic of manure and sewage. Because of the connection of surface waters to the shallow groundwater system, the potential influx from these NO_3-impacted rivers contributes manure- and sewage-sourced nitrate directly to the local groundwaters.

Nitrate derived from manure can also be explained by the large amounts of animal manure used to fertilise fields within the agricultural areas. Use of animal manure is a common practice in Algeria because the Algerian Government prohibited the general use of industrial synthetic fertilizers in the 1990s (Chabour, 200; Boumaiza et al., 2020, 2019). However, the use of synthetic fertilizers was recently re-authorized. Indeed, the 2018/2019 amount of synthetic fertilizers, including NPK fertilizers integrating nitrogen, phosphorus and potassium, applied in the Plain of the El-Nil River was estimated at 517,700 kg compared to 1,167,000 kg for animal manure (Bouakkaz and Zentout, 2020). Hence, the large application of animal manure compared to synthetic fertilizer is consistent with the present results, which reveal substantial contribution of manure- and sewage-sourced nitrate to the region. Further investigations based on additional isotope tracers (e.g., $\delta^{11}B$) (Lasagna and De Luca, 2017; Re et al., 2021) or combining emerging compounds (Erostate et al., 2019) could help to distinguish sewage from animal waste sources. There is a slight positive correlation (R^2=0.5) between groundwater NO_3 concentrations and $\delta^{18}O_{H2O}$ values for some groundwater samples (Supplemental Fig. S2), which suggests that nitrate is leaching from the surface to groundwaters (Elmeknassi et al., 2022). Such leaching could occur via: (i) direct rainwater infiltration and/or during irrigation water-return that could facilitate the leaching of fertilisers added on the agricultural lands, and/or (ii) via potential impacted river influx (Malki et al., 2017; Zhang et al., 2014).

4.3 Effect of multi-stressors on groundwater quality

The combined use of stable nitrate isotopes, along with chemical analyses revealed that groundwater quality deterioration within the Plain of the El-Nil River system is the result of combined anthropogenic contamination originating from: (i) wastewater discharge into the rivers and aquifers; (ii) the high use of manure-based fertilizers on local agricultural areas; and (iii) saltwater intrusion from the Mediterranean Sea. These results show that coastal aquifers are subjected to multiple stressors constituting multiple origins of groundwater contamination, such that the combined effects of these processes can impact large regions of the coast. Ten out of 27 groundwater samples collected from the study area are affected by saltwater intrusion (37%). The other 17 groundwater samples (63%) do not appear to be affected by saltwater intrusion. Among the groundwater samples not affected by seawater intrusion, eight samples did not exhibit nitrate of anthropogenic origin, whereas nine groundwater samples are contaminated with NO_3 (5.8–75 mg/L) of anthropogenic origin, sourced chiefly from manure and sewage. Among the ten groundwater samples affected by seawater, only one sample has NO_3 concentration close to the background (i.e., NO_3 <5 mg/L), whereas the other nine groundwater samples have NO_3 concentrations ranging from 8.5 mg/L to 60 mg/L. Hence, 90% of the groundwater samples affected by seawater intrusion are also affected by NO_3 originating from anthropogenic sources. Groundwaters affected by both seawater intrusion and anthropogenic nitrate input correspond to 33% of the total of groundwater samples collected over the study area (Supplemental Fig. S3).

These results demonstrate that the combined effects of seawater intrusion and wastewater nitrate contamination affects a large proportion of the aquifer. The spatial classified groundwater distribution shown in Supplemental Fig. S4 indicates an overlapped-crossed-contaminated sector located over the northern part of the study area. The sector affected by overlapped-crossed-contamination is in the region characterised by flat terrain and low hydraulic gradients. Hence, contribution in nitrate in this sector could be supported by potential nitrate inputs from the southern part of the study area where hydraulic gradients are higher. The piezometric map (Fig. 2) shows that groundwater flows from the south toward the Mediterranean Sea in the north; a flow movement fostering advective nitrate transport towards the northern sector.

5 Conclusion

The present study combines analyses of chemical and isotopic tracers to provide a solid framework that allows for the identification of major anthropogenic sources affecting water resources in coastal agricultural areas. In this study, the analytical results of major chemical elements were integrated in HFE-D and combined with $\delta^{2}H_{H2O}$ and $\delta^{18}O_{H2O}$ to assess seawater contamination and to identify inland marine intrusion, whereas $\delta^{15}N_{NO3}$ and $\delta^{18}O_{NO3}$ in combination with NO_3/Cl versus Cl data and a MixSIAR model provided a means to elucidate nitrate sources and their apportionment in the study area. Results of this study of coastal agricultural plain of the El-Nil River (Algeria) highlight important issues affecting coastal areas including the description of key groundwater salinization processes, as well as delineating the influence seawater intrusion over the study area. Seawater intrusion in the region includes: (i) classic inland intrusion of seawater, and (ii) potential direct seawater impact through surface water of main the river debouching into the Mediterranean Sea. Furthermore, different sources of nitrate contamination were distinguished with sewage and manure constituting the main sources of nitrate to the local groundwater and surface water systems. Nitrate derived from sewage sources likely reflects seepage from private sanitation systems within the study area and from the sanitation networks that directly discharge into the rivers without pre-treatment. Nitrate derived from manure sources is explained by large amounts of animal manure used to fertilize the agricultural areas. This study highlights the importance of distinguishing NO_3 sources in groundwater even NO_3 concentrations are low; this leads to an efficient groundwater management once the NO_3 sources are constrained.

The negative impact of seawater intrusion, including salinization of freshwater resources, combined with wastewater discharges and the use of manure-based fertilizers, raise serious questions regarding the sustainability of current agricultural activities in the region. Much of the development of the entire region is, however, directly dependent on this agriculture. This situation demonstrates that combined anthropogenic sources affect a large proportion of the study area. Optimization strategies, including an introduction of environmentally safe agricultural practices and an implementation of regulations for managing wastewater, are necessary to achieve a sustainable management of this Mediterranean coastal agricultural region. Furthermore, attention should be paid to seawater contamination. In the meantime, it is recommended to perform groundwater quality monitoring over the study area to track the temporal and spatial evolution of seawater intrusion and nitrate contamination.

Acknowledgements

The authors thank Natural Sciences and Engineering Research Council of Canada that have funded this project (Grant number FGR-CRSNG 326881 held by Prof. Julien Walter). The authors also acknowledge the financial support from (i) *Décanat de la recherche et de la création* of the *Université du Québec à Chicoutimi* (Grant number DGECR/00241-2021 held by Prof. Julien Walter), and (ii) *Comité de liaison institutionnel* of the *Université du Québec à Chicoutimi* (Grant number CLI-55221 held by Dr. Lamine Boumaiza). Prof. Andrea Brookfield, from University of Waterloo (Canada), is thanked for her helpful suggestions on improving this manuscript. The authors thank the local population and farmers of Plain of the El-Nil River, who provided much relevant information about the management of their wastewater and offered free access to their private wells during fieldwork.

References

Aller, L., Bennett, T., Lehr, J.H., Petty, R.J., Hackett, G., 1987. DRASTIC : A Standardized Method for Evaluating Ground Water Pollution Potential Using Hydrogeologic Settings, NWWA/Epa-600/2-87-035. Doc. EPA/600/2-87/035. United States Environmental Protection Agency (USEPA), Washington, DC.

Amiour, S., 2015. Qualité des eaux et des sédiments de la plaine alluviale d'oued Nil (Wilaya de Jijel, NE Algérien). Master's thesis, Université de Jijel, Algérie.

Anornu, G., Abass Gibrilla, A., Adomako, D., 2017. Tracking nitrate sources in groundwater and associated health risk for rural communities in the White Volta River basin of Ghana using isotopic approach (δ15N, δ18O-NO3 and 3H). Sci. Total Environ. 603–604, 687–698.

Appelo, C.A.J., Postma, D., 2005. Geochemistry, groundwater and pollution, second edition, Geochemistry, Groundwater and Pollution. 2nd Edition, Balkema, Leiden, The Netherlands.

Arslan, H., Demir, Y., 2013. Impacts of seawater intrusion on soil salinity and alkalinity in Bafra Plain, Turkey. Environ. Monit. Assess. 185, 1027–1040.

Barry, D.A., 2016. Seawater intrusion processes, investigation and management: recent advances and future challenges. Adv. Water Resour. 3–26.

Bear, J., Cheng, A.H.D., Ouazar, D., Sorek, S., Herrera, I., 1999. Seawater Intrusion in Coastal Aquifers-Concepts, Methods and Practices, Seawater Intrusion in Coastal Aquifers - Concepts, Methods and Practices. Kluwer Academic Publisher, Dordrecht, Boston, London.

Bechkit, M.A., 2005. Étude hydrogéologique de la plaine d'oued Nil. Engineer's thesis, Université de Constantine, Algérie.

Berkane, S., 2011. Contribution à l'étude hydrogéologique & hydrochimique de la plaine alluviale d'oued Nil. Wilaya de Jijel. Master's thesis, Université de Constantine, Algérie.

Blaisdell, J., Turyk, M.E., Almberg, K.S., Jones, R.M., Stayner, L.T., 2019. Prenatal exposure to nitrate in drinking water and the risk of congenital anomalies. Environ. Res. 176, 1–10.

Blarasin, M., Cabrera, A., Ioannis Matiatos, I., Becher Quinodóz, F., Giuliano Albo, J., Lutri, V., Matteoda, E., Panarello, H., 2020. Comparative evaluation of urban versus agricultural nitrate sources and sinks in an unconfined aquifer by isotopic and multivariate analyses. Sci. Total Environ. 741, 1–15.

Böttcher, J., Strebel, O., Voerkelius, S., Schmidt, H.L., 1990. Using isotope fractionation of nitrate-nitrogen and nitrate-oxygen for evaluation of microbial denitrification in a sandy aquifer. J. Hydrol. 114, 413–424.

Bouakkaz, R., Zentout, W., 2020. Impact des activités agricoles sur l'environnement; cas de la plaine alluviale d'oued Nil (Jijel N-E Algérien). Master's thesis, Université de Jijel, Algérie.

Boufekane, A., 2017. Hydrologie et hydrogéologie de la région de Jijel Etude de la pollution des nappes et méthodologie de protection des ressources. Ph.D thesis, Université des Sciences et de la Technologie Houari Boumediene, Alger, Algérie.

Boufekane, A., Saibi, H., Saighi, O., 2019. Comparison of TwoMethods for Groundwater Pollution Intrinsic Vulnerability Mapping in Wadi Nil (Jijel, North-East Algeria), in: Chaminé H., Barbieri M., Kisi O., Chen M., Merkel B. (Eds) Advances in Sustainable and Environmental Hydrology, Hydrogeology, Hydrochemistry and Water Resources. CAJG 2018. Advances in Science, Technology & Innovation (IEREK Interdisciplinary Series for S. pp. 277–282.

Bouillin, J.P., Kornprobst, J., 1974. Associations ultrabasiques de Petite Kabylie; peridotites de type alpin et complexe stratifie; comparaison avec les zones internes betico-rifaines. Bull. la Soc. Geol. Fr. S7, 183–194.

Boumaiza, L., Chabour, N., Drias, T., 2019. Reviewing the potential anthropogenic sources of groundwater contamination - Case study of the expanding urban area of Taleza in Algeria, in: Proceedings of the 72nd Canadian Geotechnical Conference (GeoSt-John's 2019), Saint-John's, Newfoundland and Labrador, Canada,. p. 9.

Boumaiza, L., Chesnaux, R., Drias, T., Walter, J., Huneau, F., Garel, E., Knoeller, K., Stumpp, C., 2020. Identifying groundwater degradation sources in a Mediterranean coastal area experiencing significant multi-origin stresses. Sci. Total Environ. 746, 1–20.

Boumaiza, L., Chesnaux, R., Walter, J., Drias, T., Huneau, F., Garel, E., Vystavna, Y., Stumpp, C., 2021. Reviewing the anthropogenic sources of groundwater contamination in the Plain of the El-Nil River, Algeria, in: Proceedings of the 74th Canadian Geotechnical Conference and the 14th Joint CGS/IAH-CNC Groundwater Conference (GeoNiagara-2021), Niagara Falls, Ontario, Canada. p. 9.

Cao, S., Fei, Y., Tian, X., Cui, X., Zhang, X., Yuan, R., Li, Y., 2021. Determining the origin and fate of nitrate in the Nanyang Basin, Central China, using environmental isotopes and the Bayesian mixing model. Environ. Sci. Pollut. Res. 28, 48343–48361.

Casciotti, K.L., Sigman, D.M., Hastings, M.G., Böhlke, J.K., Hilkert, A., 2002. Measurement of the oxygen isotopic composition of nitrate in seawater and freshwater using the denitrifier method. Anal. Chem. 74, 4905–4912.

Ceburnis, D., Rinaldi, M., Keane-Brennan, J., Ovadnevaite, J., Martucci, G., Giulianelli, L., O'Dowd, C.D., 2014. Marine submicron aerosol sources, sinks and chemical fluxes. Atmos. Chem. Phys. 14, 23847–23889.

Celle-Jeanton, H., Travi, Y., Blavoux, B., 2001. Isotopic typology of the precipitation in the Western Mediterrenean region at the three different time scales. Geophys. Res. Lett. 28, 1215–1218.

Celle, H., 2000. Caractérisation des précipitations sur le pourtour de la Méditerranée occidentale. Approche isotopique et chimique. PhD thesis, Université d'Avignon,

France.
CGG, (Compagnie Générale de Géophysique), 1971. Étude géophysique des plaines de Nil, Djendjen et Mencha (Jijel). Service du génie rural et de l'hydraulique agricole, Arrondissement de Constantine, Algérie.
Chabour, N., 2004. La surexploitation des eaux souterraines dans les plaines littorales : la nappe de Télezza dans la plaine de Collo (Nord-Est algérien). Sci. Technol. 127–132.
Chafouq, D., El Mandour, A., Elgettafi, M., Himi, M., Chouikri, I., Casas, A., 2018. Hydrochemical and isotopic characterization of groundwater in the Ghis-Nekor plain (northern Morocco). J. African Earth Sci. 139, 1–13.
Chesnaux, R., Marion, D., Boumaiza, L., Richard, S., Walter, J., 2021. An analytical methodology to estimate the changes in fresh groundwater resources with sea-level rise and coastal erosion in strip-island unconfined aquifers: illustration with Savary Island, Canada. Hydrogeol. J. 29, 1355–1364.
Craig, H., 1961. Isotopic variations in meteoric waters. Science (80-.). 133, 1702–1703.
Dhakate, R., Venkata Ratnalu, G., Sankaran, S., 2020. Hydrogeochemical and isotopic study for evaluation of seawater intrusion into shallow coastal aquifers of Udupi District, Karnataka, India. Geochemistry 80, 1–12.
Drouiche, A., Zahi, F., Debieche, T.H., Lekoui, A., Mahdid, S., 2022. Assessment of surface water quality: a case of Jijel region, North-East Algeria. Arab. J. Geosci. 15, 1–18.
Durand, D.M., 1969. Mise au point sur la structure du nord-est de la Berberie. Bull. du Serv. Géologique l'Algérie 39, 89–131.
Durozoy, G., 1954. Esquisse géologique au 1/50 000 de la région de Jijel. Bulletin des cartes géologiques-Publication Service.
Elmeknassi, M., Bouchaou, L., El Mandour, A., Elgettafi, M., Himi, M., Casas, A., 2022. Multiple stable isotopes and geochemical approaches to elucidate groundwater salinity and contamination in the critical coastal zone: A case from the Bou-areg and Gareb aquifers (North-Eastern Morocco). Environ. Pollut. 300, 1–13.
Erisman, J.W., Sutton, M.A., Galloway, J., Klimont, Z., Winiwarter, W., 2008. How a century of ammonia synthesis changed the world. Nat. Geosci. 1, 636–639.
Erostate, M., Huneau, F., Garel, E., Lehmann, M.F., Kuhn, T., Aquilina, L., Vergnaud-Ayraud, V., Labasque, T., Santoni, S., Robert, S., Provitolo, D., Pasqualini, V., 2018. Delayed nitrate dispersion within a coastal aquifer provides constraints on land-use evolution and nitrate contamination in the past. Sci. Total Environ. 644, 928–940.
Erostate, M., Huneau, F., Garel, E., Vystavna, Y., Santoni, S., Pasqualini, V., 2019. Coupling isotope hydrology, geochemical tracers and emerging compounds to evaluate mixing processes and groundwater dependence of a highly anthropized coastal hydrosystem. J. Hydrol. 578, 1–22.
Foster, S.S.D., Chilton, P.J., 2003. Groundwater: the processes and global significance of aquifer degradation. Philos. Trans. R. Soc. Biol. Sci. 358, 1957–1972.
Freney, E., Sellegri, K., Nicosia, A., Williams, L.R., Rinaldi, M., Trueblood, J.T., Prévôt, A.S.H., Thyssen, M., Grégori, G., Haëntjens, N., Dinasquet, J., Obernosterer, I., Wambeke, F.V., Engel, A., Zäncker, B., Desboeufs, K., Asmi, E., Timonen, H., Guieu, C., 2021. Mediterranean nascent sea spray organic aerosol and relationships with seawater biogeochemistry. Atmos. Chem. Phys. 21, 10625–10641.
Gat, J.R., Carmi, I., 1970. Evolution of the isotopic composition of the atmospheric water

in the Mediterranean Sea area. J. Geophys. Reseach 75, 3039–3048.

Gibbs, R.J., 1970. Mechanisms controlling world water chemistry. Science (80-.). 170, 1088–1090.

Gilabert-Alarcón, C., Daesslé, L.W., Salgado-Méndez, S.O., Pérez-Flores, M.A., Knöller, K., Kretzschmar, T.G., Stumpp, C., 2018. Effects of reclaimed water discharge in the Maneadero coastal aquifer, Baja California, Mexico. Appl. Geochemistry 92, 121–139.

Giménez-Forcada, E., 2010. Dynamic of sea water interface using hydrochemical facies evolution diagram. Ground Water 48, 212–216.

Giménez-Forcada, E., Sánchez San Román, F.J., 2015. An Excel Macro to Plot the HFE-Diagram to Identify Sea Water Intrusion Phases. Groundwater 53, 819–824.

Gomez Isaza, D.F., Cramp, R.L., Franklin, C.E., 2020. Living in polluted waters: A meta-analysis of the effects of nitrate and interactions with other environmental stressors on freshwater taxa. Environ. Pollut. 261, 1–12.

He, S., Li, P., Su, F., Wang, D., Ren, X., 2022. Identification and apportionment of shallow groundwater nitrate pollution in Weining Plain, northwest China, using hydrochemical indices, nitrate stable isotopes, and the new Bayesian stable isotope mixing model (MixSIAR). Environ. Pollut. 298, 1–11.

Hounslow, A.W., 1995. Water quality data: Analysis and interpretation. Boca Raton, FL: Lewis.

IAEA, (International Atomic Energy Agency), 2021. IAEA's scientific, technical and regulatory information resources. https://nucleus.iaea.org/Pages/default.aspx.

Kaown, D., Koh, E.H., Mayer, B., Ju, Y., Kim, J., Lee, H.L., Lee, S.S., Park, D.K., Lee, K.K., 2021. Differentiation of natural and anthropogenic contaminant sources using isotopic and microbial signatures in a heavily cultivated coastal area. Environ. Pollut. 273, 1–13.

Kendall, C., 1998. Tracing Nitrogen Sources and Cycling in Catchments. Isot. Tracers Catchment Hydrol. 519–576.

Kendall, C., Elliott, E.M., Wankel, S.D., 2007. Tracing Anthropogenic Inputs of Nitrogen to Ecosystems, Chapter 12, In: R.H. Michener and K. Lajtha (Eds.). Stable Isot. Ecol. Environ. Sci. Second Ed. Blackwell Publ. 375–449.

Kwon, E., Park, J., Park, W.B., Kang, B.R., Woo, N.C., 2021. Nitrate contamination of coastal groundwater: Sources and transport mechanisms along a volcanic aquifer. Sci. Total Environ. 768, 1–11.

Lasagna, M., De Luca, D.A., 2017. Evaluation of sources and fate of nitrates in the western Po plain groundwater (Italy) using nitrogen and boron isotopes. Environ. Sci. Pollut. Res. 26, 2089–2104.

Letouzey, J., Trémolières, P., 1980. Paleo-stress fields around the Mediterranean since the Mesozoic derived from microtectonics : comparisons with plate tectonic data data. B.R.G.M. theisis 115, 261–273.

Li, J., Zhu, D., Zhang, S., Yang, G., Zhao, Y., Zhou, C., Lin, Y., Zou, S., 2022. Application of the hydrochemistry, stable isotopes and MixSIAR model to identify nitrate sources and transformations in surface water and groundwater of an intensive agricultural karst wetland in Guilin, China. Ecotoxicol. Environ. Saf. 231, 1–11.

Madioune, D.H., Faye, S., Orban, P., Brouyère, S., Dassargues, A., Mudry, J., Stumpp, C., Maloszewski, P., 2014. Application of isotopic tracers as a tool for understanding hydrodynamic behavior of the highly exploited Diass aquifer system (Senegal). J. Hydrol. 511, 443–459.

Mahdid, S., Chabour, N., T.H., D., Drouiche, A., F., Z., S., P., 2022. Evaluation and comparison of groundwater vulnerability to pollution by the DRASTIC and GOD methods: a case of Wadi Nil alluvial plain (Jijel, NE Algeria). Food Environ. Saf. 1, 62–75.

Mahlknecht, J., Merchán, D., Rosner, M., Meixner, A., Ledesma-Ruiz, R., 2017. Assessing seawater intrusion in an arid coastal aquifer under high anthropogenic influence using major constituents, Sr and B isotopes in groundwater. Sci. Total Environ. 587–588, 282–295.

Malki, M., Bouchaou, L., Hirich, A., Ait Brahim, Y., Choukr-Allah, R., 2017. Impact of agricultural practices on groundwater quality in intensive irrigated area of Chtouka-Massa, Morocco. Sci. Total Environ. 574, 760–770.

Matiatos, I., 2016. Nitrate source identification in groundwater of multiple land-use areas by combining isotopes and multivariate statistical analysis: A case study of Asopos basin (Central Greece). Sci. Total Environ. 541, 802–814.

Mengis, M., Schiff, S.L., Harris, M., English, M.C., Aravena, R., Elgood, R.J., MacLean, A., 1999. Multiple geochemical and isotopic approaches for assessing ground water NO3 - Elimination in a riparian zone. Ground Water 37, 448–457.

Merchan, D., Sanz, L., Alfaro, A., P erez, I., Goni, M., Solsona, F., Hernandez-García, I., P erez, C., Casalí, J., 2020. Irrigation implementation promotes increases in salinity and nitrate concentration in the lower reaches of the Cidacos River (Navarre, Spain). Sci. Total Environ. 706, 1–11.

Messadi, H., 1992. Synthèse de données hydrochimiques des plaines alluviales des oueds : Nil, Djendjen et Mencha. Master’s thesis, Université de Constantine, Algérie.

Obeidat, M., Awawdeh, M., I., M., Al-Ajlouni, A., Al-Mughaid, H., 2021. Identification and apportionment of nitrate sources in the phreatic aquifers in Northern Jordan using a dual isotope method (δ15N and δ18O of NO3-). Groundw. Sustain. Dev. 12, 1–13.

Panno, S.V., Kelly, W.R., Martinsek, A.T., Hackley, K.C., 2006. Estimating background and threshold nitrate concentrations using probability graphs. Ground Water 44, 697–709.

Parnell, A.C., Inger, R., Bearhop, S., Jackson, A.L., 2010. Source partitioning using stable isotopes: coping with too much variation. PLoS One 5(3):e9672. https://doi.org/10.1371/journal.pone.0009672

Pastén-Zapata, E., Ledesma-Ruiz, R., Harter, T., Ramírez, A.I., Mahlknecht, J., 2014. Assessment of sources and fate of nitrate in shallow groundwater of an agricultural area by using a multi-tracer approach. Sci. Total Environ. 855–864.

Penna, D., Stenni, B., Šanda, M., Wrede, S., Bogaard, T.A., Gobbi, A., Borga, M., Fischer, B.M.C., Bonazza, M., Chárová, Z., 2010. On the reproducibility and repeatability of laser absorption spectroscopy measurements for δ 2 H and δ 18 O isotopic analysis. Hydrol. Earth Syst. Sci. 14, 1551–1566.

Piper, A.M., 1944. A graphic procedure in the geochemical interpretation of water-analyses. Eos, Trans. Am. Geophys. Union 25, 914–928.

Puig, R., Soler, A., Widory, D., Mas-Pla, J., Domènech, C., Otero, N., 2017. Characterizing sources and natural attenuation of nitrate contamination in the BaixTer aquifer system (NE Spain) using a multi-isotope approach. Sci. Total Environ. 580, 518–532.

Pulido-Bosch, A., Rigol-Sanchez, J.P., Vallejos, A., Andreu, J.M., Ceron, J.C., Molina-Sanchez, L., Sola, F., 2018. Impacts of agricultural irrigation on groundwater salinity. Environ. Earth Sci. 77, 1–14.

Re, E., Sacchi, E., Mas-Pla, J., Mencio, A., El-Amrani, N., 2014. Identifying the effects of human pressure on groundwater quality to support water management strategies in coastal regions: A multi-tracer and statistical approach (Bou-Areg region, Morocco). Sci. Total Environ. 500–501, 211–223.

Re, V., Kammoun, S., Sacchi, E., Trabelsi, R., Zouari, K., Matiatos, I., Allais, E., Daniele, S., 2021. A critical assessment of widely used techniques for nitrate source apportionment in arid and semi-arid regions. Sci. Total Environ. 775, 1–12.

Re, V., Sacchi, E., 2017. Tackling the salinity-pollution nexus in coastal aquifers from arid regions using nitrate and boron isotopes. Environ. Sci. Pollut. Res. 24, 13247–13261.

Santoni, S., Huneau, F., GAREL, E., Celle-Jeanton, H., 2018. Multiple recharge processes to heterogeneous Mediterranean coastal aquifers and implications on recharge rates evolution in time. J. Hydrol. 559, 669–683.

Schroeder, A., Souza, D.H., Fernandes, M., Rodrigues, E.B., Trevisan, V., Skoronski, E., 2020. Application of glycerol as carbon source for continuous drinking water denitrification using microorganism from natural biomass. J. Environ. Manage. 256, 109964–109971.

Shi, L., Jiao, J.J., 2014. Seawater intrusion and coastal aquifer management in China: a review. Environ. Earth Sci. 27, 2811–2819.

Sigman, D.M., Casciotti, K.L., Andreani, M., Barford, C., Galanter, M., Böhlke, J.K., 2001. A bacterial method for the nitrogen isotopic analysis of nitrate in seawater and freshwater. Anal. Chem. 73, 4145–4153.

Singleton, M.J., Esser, B.K., Moran, J.E., Hudson, G.B., Mcnab, W.W., Harter, T., 2007. Saturated zone denitrification: Potential for natural attenuation of nitrate contamination in shallow groundwater under dairy operations. Environ. Sci. Technol. 41, 759–765.

Stock, B.C., Jackson, A.L., Ward, E.J., Parnell, A.C., Phillips, D.L., Semmens, B.X., 2018. Analyzing mixing systems using a new generation of Bayesian tracer mixing models. PeerJ 6, e5096. https://doi.org/https://doi.org/10.7717/peerj.5096.

Stoewer, M.M., Knöller, K., Stumpp, C., 2015. Tracing freshwater nitrate sources in pre-alpine groundwater catchments using environmental tracers. J. Hydrol. 524, 753–767.

Sutton, M.A., Howard, C.M., Erisman, J.W., Billen, G., Bleeker, A., Grennfelt, P., Van Grinsven, H., Grizzetti, B., 2011. The European Nitrogen Assessment, The European Nitrogen Assessment. Cambridge University Press.

Torres-Martínez, J.A., Mora, A., Mahlknecht, J., Daessle, L.W., Cervantes-Aviles, P.A., Ledesma-Ruiz, R., 2021. Estimation of nitrate pollution sources and transformations in groundwater of an intensive livestock-agricultural area (Comarca Lagunera), combining major ions, stable isotopes and MixSIAR model. Environ. Pollut. 269, 1–12.

Vila, J.M., 1980. La chaîne alpine d'Algérie orientale et des confins Algéro-tunisiens. Ph.D thesis, Université de Pierre et Marie- Curie, France.

Vystavna, Y., Diadin, D., Yakovlev, V., Hejzlar, J., Vadillo, I., Huneau, F., Lehmann, M.F., 2017. Nitrate contamination in a shallow urban aquifer in East Ukraine: evidence from hydrochemical, stable isotopes of nitrate and land use analysis.

Environ. Earth Sci. 76, 1–13.

Ward, M., Jones, R., Brender, J., De Kok, T., Weyer, P., Nolan, B., Van Breda, S., 2018. Drinking water nitrate and human health: an updated review. Int. J. Environ. Res. Public Health 15, 1–31.

Wassenaar, L.I., 1995. Evaluation of the origin and fate of nitrate in the Abbotsford Aquifer using the isotopes of15N and18O in NO3-. Appl. Geochemistry 10, 391–405.

WHO, (World Health Organization), 2017. Guidelines for drinking-water quality, 4th edition, incorporating the 1st addendum. ISBN: 978-92-4-154995-0.

Yeshno, E., Arnon, S., Dahan, O., 2019. Real-time monitoring of nitrate in soils as a key for optimization of agricultural productivity and prevention of groundwater pollution. Hydrol. Earth Syst. Sci. 23, 3997–4010.

Zendehbad, M., Cepuder, P., Loiskandl, W., Stumpp, C., 2019. Source identification of nitrate contamination in the urban aquifer of Mashhad, Iran. J. Hydrol. Reg. Stud. 25, 1–14.

Zhang, Y., Li, F., Zhang, Q., Li, J., Liu, Q., 2014. . Tracing nitrate pollution sources and transformations in surface- and ground-waters using environmental isotopes. Sci. Total Environ. 490, 213–222.